Using nitroxide spin labels

How to obtain T_{1e} from continuous wave electron paramagnetic resonance spectra at all rotational rates

D. A. Haas, C. Mailer, and B. H. Robinson
Chemistry Department, University of Washington, Seattle, Washington 98195 USA

ABSTRACT Historically, the continuous wave electron paramagnetic resonance (CW-EPR) progressive saturation method has been used to obtain information on the spin-lattice relaxation time (T_{1e}) and those processes, such as motion and spin exchange, that occur on a competitive timescale. For example, qualitative information on local dynamics and solvent accessibility of proteins and nucleic acids has been obtained by this method. However, making quantitative estimates of T_{1e} from CW-EPR spectra have been frustrated by a lack of understanding of the role of T_{1e} (and T_{2e}) in the slow-motion regime. Theoretical simulation of the CW-EPR lineshapes in the slow-motion region under increasing power levels has been used in this work to test whether the saturation technique can produce *quantitative* estimates of the spin-lattice relaxation rates. A method is presented by which the correct T_{1e} may be extracted from an analysis of the power-saturation rollover curve, regardless of the amount of inhomogeneous broadening or the rates of molecular reorientation. The range of motional correlation times from 10 to 200 ns should be optimal for extracting quantitative estimates of T_{1e} values in spin-labeled biomolecules. The progressive-saturation rollover curve method should find wide application in those areas of biophysics where information on molecular interactions and solvent exposure as well as molecular reorientation rates are desired.

INTRODUCTION

The aim of this article is to determine whether the power saturation method of continuous wave electron paramagnetic resonance (CW-EPR) can be used to determine relaxation times of nitroxide spin labels. In the fast-motion limit where the EPR lines are homogeneously broadened, the standard saturation theory used to obtain T_{1e} and T_{2e} is well known and simple to apply (1, 2). However, as the motion slows the lines become inhomogeneously broadened because anisotropies in the g- and A-tensors are no longer completely averaged away, and the simple theory breaks down. A large body of work exists to analyze inhomogeneous lineshapes, primarily in the EPR of solids. To the best of our knowledge, virtually all previous work assumes some form of distribution of the individual, homogeneous resonance lines that is static on the time scale of the EPR measurement (3–5). Some treatments do allow spin diffusion (6, 7) but still assume Gaussian or Lorentzian line shapes. Freed and co-workers (8, 9) have studied saturation in liquids and demonstrated the line broadening effects of high microwave powers. The present treatment extends previous theoretical developments to show how a saturation curve may be used to obtain T_{1e} in an experimental situation.

The primary motivation for this article lies in the recent work of Altenbach et al. (10), who used changes in the apparent relaxation rates of spin labels to determine molecular structure. A label at a known position in a molecule that has some contact with a spin relaxing agent will have a faster relaxation rate compared with a control with no such relaxing agent. Relaxation rates were not measured directly, but were obtained by CW power saturation of the first-derivative EPR signal. The CW-EPR signal height, when measured as a function of incident microwave power, rises to a maximum and then decreases. The incident power level at which the signal is reduced by 3 dB is called the "half-power" saturation parameter, $P_{1/2}$, and Altenbach et al. (10) used this quantity as a measure of the relaxation rate. Altenbach et al. determined the α-helical nature of a *trans*-membrane protein from the periodicity of the $P_{1/2}$ of a spin label selectively attached to a single amino acid sidechain in the sequence. The spin label relaxation rate increased for those amino acids that were in contact with an oxygen-rich lipid environment.

One assumption in simple theories of the relation between $P_{1/2}$ and the relaxation rate is that the line measured is a single, homogeneous one. In general, the spectral lines are very definitely not homogeneous, being a complex mixture of partially averaged tensors and dynamical interactions, because the labels are moving in the nanosecond motional region. Nevertheless, the relative changes in $P_{1/2}$ produced a plausible map of lipid accessibility. We wish to understand why the saturation method worked as well as it did and to determine whether there are any improvements that can be made in the methodology of the experiments. In particular, we wish to know whether the true spin–lattice relaxation time (in agreement with that measured by saturation recovery EPR) and the true spin–spin relaxation time can be obtained from power saturation studies when the motion is in the nanosecond regime. To do this we have computed EPR spectra of an ^{14}N spin label over a wide range of microwave powers at various rotational correlation times and have analyzed the results. There are no assumptions about the distribution function of the inho-

Address correspondence to Dr. Bruce H. Robinson, Department of Chemistry, Room BG-10, University of Washington, Seattle, WA 98195, USA.

0006-3495/93/03/594/11 $2.00

mogeneous broadening. The EPR simulation programs developed by us (11, 12) (originally for saturation transfer [ST]-EPR) explicitly include the A- and g-tensors, motion, the Zeeman modulation frequency, and the relaxation times.

THEORY

The spectra were calculated by solving the spin density matrix equation that explicitly includes rf field levels, relaxation times, Zeeman modulation, and the correlation time for isotropic rotational Brownian motion of the label (11, 12). The equation of motion of the density matrix is:

$$\dot{\sigma}(\Omega, t) = -i[H(\Omega, t), \sigma(\Omega, t)] - \Gamma_R\{\sigma(\Omega, t) - \sigma^0(\Omega, t)\} - \Gamma_\Omega\{\sigma(\Omega, t) - \sigma^0(\Omega, t)\}, \quad (1)$$

where $\sigma(\Omega, t)$ is the spin density matrix, $H(\Omega, t)$ is the spin Hamiltonian, and Γ_Ω is a Markoffian motional operator affecting only the orientation variable Ω. Γ_R describes spin relaxation arising from the modulation of spatial coordinates other than Ω, via a phenomenological fast-motion or Redfield type matrix, and includes T_{1e} and T_{2e}^0 (13)—entered directly into the program—and $\sigma^0(\Omega, t)$, the equilibrium density matrix.[1] The Hamiltonian $H(\Omega, t)$ may be expressed as:

$$H(\Omega, t) = \mathscr{H}_0 + \mathscr{H}_1(\Omega) + \epsilon(t),$$

where the orientation-independent Hamiltonian is given by:

$$\mathscr{H}_0 = \gamma_e H_0 S_z - \gamma_n H_0 I_z + \gamma_e \bar{a}[S_z I_z], \quad (2)$$

including isotropic electron Zeeman, nuclear Zeeman, and electron-nuclear hyperfine interactions. γ_e and γ_n are the electron and nuclear gyromagnetic ratios, H_0 is the DC Zeeman field and $\bar{a}$ is the isotropic hyperfine interaction. $\mathscr{H}_1(\Omega)$ is the time-independent but orientation-dependent Hamiltonian and is given in detail elsewhere (11). $\mathscr{H}_1(\Omega)$ is dependent on the anisotropies of the A (the electron-nuclear hyperfine) and g (the electron Zeeman) tensors as well as the rotation angles, Ω, written in terms of the Wigner rotational matrix elements. The principal axes of the A- and g-tensors are assumed to be coincident. $\mathscr{H}_1(\Omega)$ modifies the resonance position due to the orientation of the molecule, and it is this term that gives rise to asymmetries in the spectra when the motion is slow. When the motion is fast enough to average each manifold to a single line, then $\mathscr{H}_1(\Omega)$ and Γ_Ω may be removed from Eq. 1 and used to compute the linewidth by fast-motion (Redfield) theory. The relaxation rate and time, predicted by fast-motion theory (13), are $R_{2e}^G(m) = [T_{2e}^G(m)]^{-1}$. The contribution of $\mathscr{H}_1(\Omega)$ to the linewidth may be estimated as:

$$R_{2e}^G(m)\langle S_+\rangle = \int_0^\infty \langle |[\overline{\mathscr{H}_1(\Omega)^x, [\mathscr{H}_1(\Omega)}, S_+]]| \rangle \, dt, \quad (3)$$

where $\mathscr{H}_1(\Omega)$ in the rotating frame is:

$$\mathscr{H}_1(\Omega)^x = e^{-i\mathscr{H}_{0r}} \mathscr{H}_1(\Omega) e^{+i\mathscr{H}_{0r}}.$$

The equation for the relaxation rate predicted from simple fast-motion theory is given by Goldman et al. (14) (see Appendix). The total linewidth in the absence of inhomogeneous broadening is then predicted to be:

$$R_{2e}(m) = [T_{2e}(m)]^{-1} = R_{2e}^G(m) + [T_{2e}^0]^{-1}, \quad (4)$$

where an additional contribution to relaxation is specified only by T_{2e}^0 (13). Eq. 4 is valid for $m = 0$ or ± 1 for the ^{14}N and $m = \pm 1/2$ for the ^{15}N spin label.

The time-dependent but orientation-independent Hamiltonian $\epsilon(t)$ describes the interaction of the spins with the rf radiation and the low frequency modulation of the DC field:

$$\epsilon(t) = d_0(S_+ e^{-i\omega_0 t} + S_- e^{+i\omega_0 t}) + d_m S_z(e^{-i\omega_m t} + e^{+i\omega_m t}),$$

where ω_0 and ω_m are the frequencies of the microwave observing field of amplitude h_1 and Zeeman modulation field, of amplitude h_m, respectively. $d_0 = \frac{1}{2}\gamma_e h_1$ and $d_m = \frac{1}{2}\gamma_e h_m$ are in frequency units. The matrix elements of σ are computed using the eigenfunctions of $\mathscr{H}_0$ as a basis set. The observed signal is the deviation from equilibrium, $\chi = \sigma - \sigma^0$ (11). In the high-field and high-temperature approximation the equilibrium spin density matrix is:

$$\sigma^0 = \{N^{-1} - q[\mathscr{H}_0 + \mathscr{H}_1(\Omega)]\}P^0(\Omega),$$

and $q = \hbar/NkT$, $P^0(\Omega)$ is the equilibrium orientation distribution (assumed isotropic) and N is the number of spin states (six for ^{14}N and four for ^{15}N). These equations were programmed and solved for ^{14}N spin labels on a DEC workstation (12). Note that all of the terms in the above equations used to calculate the CW-EPR spectra are, of necessity, stationary in the rotating frame. This means that none of the terms can generate a relaxation process for T_{1e} (terms that are nonstationary in the rotating frame are needed to produce a T_{1e}). T_{1e} therefore is added into the equations via the phenomenological Redfield relaxation matrix, Γ_R, in Eq. 1.

LINESHAPE ANALYSIS

The conventional CW-EPR experiment detects the absorption signal, M_y^1, at the first harmonic of the low frequency modulation frequency. In the picosecond corre-

[1] T_{2e}^0 is the contribution to the linewidth from mechanisms not specified in the Hamiltonian. In this case it may arise from rapid fluctuations of the non-secular terms. It may be thought of as the intrinsic linewidth of the powder pattern in the absence of rotational motion. For spin labels one typically finds $20 < T_{2e}^0 < 150$ ns.

lation time fast-motion limit ^{14}N spin label absorption spectra consist of three narrow lines, whose amplitudes are given by (2):

$$M_y^1 = q\gamma_e h_m h_1 \left\{ \frac{2\Delta/T_{2e}}{(\Delta^2 + 1/S_0T_{2e}^2)(\Delta^2 + 1/S_1T_{2e}^2)} \right\}, \quad (5)$$

where

$$S_r = \left(1 + \frac{(\gamma_e h_1)^2 T_{2e} T_{1e}}{1 + (rT_{1e}\omega_m)^2} \right)^{-1}, \quad (6)$$

and $r = 0, 1, 2, 3 \cdots$ is an index that refers to the harmonic of the modulation; Δ is the frequency offset from the center of resonance. In the very fast-motion limit (picosecond correlation times), the spin–spin relaxation time is T_{2e}^0. As the motion slows, T_{2e}^0 is replaced by the $T_{2e}(m)$ given in Eq. 4. When $\omega_m T_{1e} \ll 1$, then $S_1 \approx S_0$ and $S_0 = \{1 + (\gamma_e h_1)^2 T_{2e} T_{1e}\}^{-1}$, which is the usual saturation parameter (1).[2] In this situation, the equation reduces to the familiar derivative of a Lorentzian line:

$$M_y^1 = q\gamma_e h_m h_1 \left\{ \frac{2\Delta/T_{2e}}{(\Delta^2 + 1/S_0T_{2e}^2)^2} \right\}. \quad (7)$$

The values of Δ at which the peaks of the derivative occur are at $\Delta_{max} = \pm 1/(T_{2e}\sqrt{3S_0})$. The peak-to-peak width of the line in gauss, L, is given by:

$$L^2 = L_0^2 + \frac{4}{3} h_1^2 \left(\frac{T_{1e}}{T_{2e}} \right), \quad (8)$$

where L_0 is the peak-to-peak width in the limit of very low microwave field, i.e., $L_0 = 2/(\sqrt{3}T_{2e}\gamma_e)$. Defining ΔY as the base-to-peak height of M_y^1 and substituting the values of Δ_{max} into Eq. 7 for M_y^1 gives:

$$\Delta Y = 0.7 \times q\gamma_e h_m h_1 T_{2e}^2 S_0^{3/2}.$$

At low powers, S_0 is approximately unity and the signal is proportional to h_1. As h_1 increases, S_0 decreases, and the signal levels off. At still higher levels of h_1, the term in S_0 dominates and the signal decreases, eventually becoming proportional to $1/h_1^2$. The peak-to-peak height will be maximized when $h_1 = 1/\sqrt{2\gamma_e^2 T_{1e} T_{2e}}$ and $S_0 = 2/3$. The experimental variable is the microwave power incident on the sample, P_0, and this is related to h_1 by the equation $h_1 = \alpha\sqrt{P_0}$, where α is the power to rf field conversion factor that is a function of the resonator and sample used. The relation of signal to microwave power is now in the standard form (1, 2, 15):

$$\Delta Y = \frac{cP_0^{1/2}}{(1 + P_0/P_2)^\epsilon}, \quad (9)$$

where c is an (adjustable) gain constant, and ϵ is a parameter to take account of the lineshape: $\epsilon = 3/2$ for a homogeneous first-derivative absorption line, is unity for a zero derivative absorption line (3), and is $1/2$ for a completely inhomogeneous derivative absorption line. P_2 is a saturation parameter (in units of Watts) and is defined as:

$$P_2 = [(\gamma_e \alpha)^2 T_{1e} T_{2e}]^{-1}. \quad (10)$$

Eqs. 9 and 10 are central to the analysis to obtain T_{1e} – P_2 is obtained from Eq. 9 and T_{1e} is calculated from Eq. 10, provided an estimate of T_{2e} can be obtained. It is the correct value of T_{2e} to use that has been the major problem in previous analyses. If the EPR lines are pure Lorentzians, then T_{2e} is easily found from the linewidth; most experimental spectra have much more complicated lineshapes, and the correct T_{2e} value is not obvious. We believe that this situation can be solved by combining the ϵ parameter of Eq. 9 with a linewidth measured from the spectrum to obtain an estimate of the correct "T_{2e}" to use in Eq. 10. The next few paragraphs justify the use of ϵ in this endeavor.

Fig. 1 shows the shape of the line at the low field turning point of the first harmonic EPR spectrum. It is anticipated that the saturation characteristics of this low field turning point should be those of a first harmonic (or first-derivative) Lorentzian absorption line ($\epsilon = 3/2$). When in the fast-motion limit (Fig. 1, *top*) and approximately those of a zeroth-derivative Lorentzian absorption line ($\epsilon = 1$) in the near no-motion limit (Fig. 1, *bottom*). To go smoothly from the fast-motion limit to the slow-motion limit, it seems reasonable therefore that we let ϵ be an adjustable parameter. Often the maximum of the rollover curve, P_{max}, is of interest. From Eq. 9 it follows that $P_{max} = P_2/(2\epsilon - 1)$. The $P_{1/2}$ parameter used by Altenbach et al. (10) is defined as the intersection of a straight line $\Delta Y_0 = (c/2)P_0^{1/2}$, with the curve defined by Eq. 9. The intersection of these two lines occurs when $P_{1/2} = P_2(2^{1/\epsilon} - 1)$. For the special case of a pure absorption line where $\epsilon = 1$, then $P_{1/2} = P_{max} = P_2$, but otherwise the three quantities are all slightly different. We consider P_2 to be the preferred parameter for analysis because it is independent of ϵ; P_{max} and $P_{1/2}$ clearly depend on ϵ.

Protons (or deuterons) surrounding the spin label N-O moiety cause unresolved broadening. To account for this effect, the calculated spectra were convolved with a Gaussian function and subsequently analyzed with Eq. 9. The value of ϵ is influenced by the degree of homogeneity of the EPR line (15). Its value ranges from $3/2$ for a single homogeneous line to $1/2$ for a completely inhomogeneous line. The amount of broadening for protons (deuterons) is around 0.5 (0.17) G in the fast-motion limit and around 2.8 (0.9) G in the slow motion limit (16). The nonbroadened simulated lines had width < 1 G at the fast-motion limit and several gauss in the slow motion limit, hence we expect ϵ to be changed when we perform the convolution.

[2] Poole provides the definition of the S_o parameter on p. 590 of (1).

TABLE I **The *A* and *g*-tensors and the three relative turning points for each nuclear manifold**

	X	*Y*	*Z*
A	6	6	31
g	2.0086	2.0066	2.0032
$m = -1$	1.76	5.15	35.91
$m = 0$	−4.24	−0.85	4.91
$m = +1$	−10.24	−6.85	−26.09

$m = +1$ (low field), $m = 0$ (center field), $m = -1$ (high field). *A*-tensor elements and turning points are in gauss.

It is our aim to show that Eq. 9 for the saturation rollover curve is robust enough to give a good accounting of the power dependence of the EPR signal regardless of the correlation time or the amount of proton (or deuteron) broadening. Changes in the shape of the saturation curve show up as changes in the values of ϵ and P_2.

A way to roughly estimate $1/T_{2e}$ from the spectrum, regardless of the motional rate, would be to use the width at half-peak height, W, on the tail of the Lorentzian (see Fig. 1). For a Lorentzian first harmonic (or derivative) spectrum with $\epsilon = 3/2$, we find that $W = 0.809/\gamma_e T_{2e} \cong 1/\sqrt{\epsilon}\gamma_e T_{2e}$. The zeroth-derivative absorption Lorentzian ($\epsilon = 1.0$) yields $W = 1/\gamma_e T_{2e}$. $R_w \equiv 1/T_{2e}$ is an effective linewidth that takes into account the lineshape changes that occur as the motional rate changes, and is defined as:

$$R_w = 1/T_{2e} \approx \sqrt{\epsilon}\gamma_e W, \qquad (11)$$

where W is obtained when h_1 is so small that no saturation is present.

Under saturation conditions, lines broaden, and Eq. 8 shows how the line width, L, depends on the observer amplitude. A linear plot of L^2 vs. h_1^2 has been used as a means of calibrating h_1 (17) and can give T_{1e} provided T_{2e} is known. This method works well at fast motions typical of the spectra in Fig. 1 (*top*) and could, in principle, be used to analyze the data at slower correlation times (2). However, it failed in practice because the plots were nonlinear. Furthermore, there was no parameter analogous to ϵ that could take account of shape changes in a simple way.

METHODS

(*a*) The EPR spectra were simulated for different values of the incident observer amplitude, h_1, with a fixed set of parameters. Table 1 presents the *A*- and *g*-tensors used in all of the simulations, as well as the *x*, *y*, and *z* turning points for each manifold, $m = 0, \pm 1$. The values of T_{1e} and T_{2e}^0, and the isotropic, Brownian rotational reorientation with characteristic correlation time, τ_c, are in Table 2. The spectra were convolved with a Gaussian function to include the effects of protons (see Table 3).

(*b*) For a fixed set of parameters, a signal versus power rollover curve was obtained (see Fig. 2) and was fit by least-squares to a linearized version of Eq. 9:

$$[\Delta Y(P_0^{(\epsilon-1/2)})]^{1/\epsilon} = (c^{1/\epsilon}P_2) - P_2 \times [\Delta Y/P_0^{1/2}]^{1/\epsilon}, \qquad (12)$$

to obtain c (which is of no interest), ϵ, and P_2.

(*c*) For a given correlation time, P_2 versus $1/T_{1e}$ was plotted (see Fig. 3).

(*d*) The quantity R_2, equivalent to $1/T_{2e}$ for a simple Lorentzian line, can be defined by rearranging Eq. 10:

$$R_2 = P_2[(\gamma_e\alpha)^2 T_{1e}]. \qquad (13)$$

R_2 was computed for comparison with theory (Eqs. 3 and 11 and the Appendix).

Table 2 presents the results from the analysis: P_2, ϵ, R_2 for $\sigma = 0.0$ G (no convolution) and R_w (measured from W) given in Eq. 11. Table 3 shows results similar to Table 2 for spectra convolved with $\sigma = 2.0$ G. Table 3 also contains additional information about the effects of inhomogeneous broadening (vide infra).

RESULTS

Fig. 1 shows simulated lineshapes for two different correlation times. The top figure has $\tau_c = 10$ ps (chosen for comparison with fast-motion theory), and the bottom one has $\tau_c = 30$ ns (a correlation time typical of spectra obtained in the experiments of Altenbach et al. [10]). The signal height for analysis, ΔY, as well as the width at half-height, W, are indicated. The spectra show the signals well below saturation and have no convolution included; in an actual experiment the lines would be further broadened by unresolved protons or deuterons on the label. Clearly, as the correlation time increases, the spectrum does not remain as three sharp homogeneous lines.

Fig. 2 is a plot of signal height ΔY versus the incident microwave power P_0 (the "rollover" saturation curve) for the spectra in Fig. 1. P_0 was calculated from h_1 as $P_0 = (h_1/\alpha)^2$ and $\alpha = 4.5$ G/$\sqrt{\text{Watt}}$, which is typical of a medical advances loop gap resonator (LGR); $\alpha = 1.5$ G/$\sqrt{\text{Watt}}$ for a standard TE_{102} cavity (2). Eq. 12 is linearized with respect to c and P_2 but requires a nonlinear search on ϵ. This equation weights the low power terms more heavily to produce a reasonable fit, as can be judged from Fig. 2. The solid lines are the best least-squares fits to the ΔY predicted by Eq. 12 and the ΔY measurements from Fig. 1.

Fig. 3 shows a plot of P_2 obtained from the rollover curves versus T_{1e}^{-1} for several fixed correlation times and T_{2e}^0. The values of T_{1e} were those entered into the simulation program in Table 2. Superimposed on the data is a least-squares best fit to the data of $P_2 = \rho T_{1e}^{-1}$, where ρ is an adjustable constant.

Fig. 4 shows the values of R_2 as a function of τ_c for different values of T_{1e} given in Table 2. In the curve on top in Fig. 4, $T_{2e}^0 = 30$ ns, and on the bottom curve, $T_{2e}^0 = 100$ ns. Also plotted is R_w given in Table 2, which is a rough estimate of R_{2e} for the low-field manifold obtained from the line's width at half height. Also shown on Fig. 4 are estimates of R_{2e} given by fast-motion relaxation theory (14), by a first-order modification to fast-motion

TABLE 2 **Input parameters for simulations and parameters of rollover curve analysis**

Input values			Results					
τ_c	T_{1e}	T_{2e}^0	ϵ	P_2	R_2	T_2	W	R_w
s	*μs*	*ns*		*mW*	*Mrad/s*	*ns*	*G*	*Mrad/s*
1E−11	0.25	30	1.465	21.3	33.41	29.9	1.55	33.02
1E−11*	0.25	100	1.489	6.33	9.94	100.6	0.405	9.96
1E−11	5	100	1.484	0.290	9.34	107.1	—	—
1E−9	0.25	30	1.34	26.9	42.15	23.7	—	—
1E−9	1	30	1.35	6.76	42.44	23.6	—	—
1E−9	5	30	1.302	1.25	39.31	25.4	2.321	46.6
1E−9	5	100	1.447	0.75	23.71	42.2	1.218	25.7
1E−8	0.25	30	1.224	92.7	145.4	6.87	—	—
1E−8	5	30	1.211	4.68	146.9	6.80	4.579	88.7
1E−8	5	100	1.224	4.27	134.2	7.45	3.522	68.6
3E−8	0.25	30	1.335	89.9	141.1	7.08	—	—
3E−8	1	30	1.325	24.4	153.4	6.51	—	—
3E−8	5	30	1.313	4.97	156.0	6.41	3.109	62.7
3E−8‡	0.25	100	1.348	71.0	111.3	8.98	—	—
3E−8	1	100	1.42	19.8	124.3	8.04	—	—
3E−8	5	100	1.329	4.10	128.6	7.77	2.062	41.8
1E−7	5	30	1.384	5.03	157.9	6.33	—	—
1E−7	15	30	1.375	1.70	160.0	6.25	2.370	48.9
1E−7	5	100	1.418	3.94	123.8	8.07	—	—
1E−7	15	100	1.417	1.36	128.2	7.79	1.314	27.5
1E−5	5	30	1.137	1.58	49.76	20.09	1.858	34.8
1E−5	5	100	1.224	0.75	23.78	42.0	0.6036	11.7

Convolution = 0 G. See Table 1 for additional input parameters. The results of ϵ and P_2 are from fitting saturation rollover curves according to Eq. 13; R_2 is calculated from Eq. 12. W is measured from the low power spectrum (see Fig. 1 for definition) and R_w is calculated from Eq. 11.
* Set of calculations used for Figs. 1 and 2, *top*.
‡ Set of calculations used for Figs. 1 and 2, *bottom*.

theory (18), and by a generalized spectral density function suggested by multiple relaxation processes (see Appendix).

DISCUSSION

Slowing of the rotational motion causes inhomogeneities due to the *g*- and *A*-tensors to become more pronounced (Fig. 1). The lineshape changes from a superposition of three homogeneous first-derivative Lorentzian shaped lines in the fast-motion limit to a complicated "powder pattern" spectrum at long correlation times. These changes in shape, especially in the center of the spectrum, cause the lines to overlap and make it difficult to estimate the height of the center line accurately. The peak height of the low field line is the best quantity to be used for a saturation rollover curve, as this place represents a spectral position that is easily identified at all motion times and is clearly associated only with a single line. This suggests that it would be better, experimentally, to use the an isotopically substituted ^{15}N nitroxide spin label rather than the ^{14}N analogue: there are only two EPR lines instead of three and the low field manifold of ^{15}N gives approximately two times bigger signal in the slow motion regime than does the ^{14}N label (19).

There is no simple a priori theory for the form of the rollover curve once one leaves the fast-motion regime. The use of Eq. 9 (or Eq. 12) to fit the rollover curve constitutes an approximation. These equations work remarkably well at fitting the results obtained directly from the simulations and continue to perform well even when Gaussian convolution is added. To obtain reliable estimates of ϵ and P_2 using Eq. 12, the rollover curves must be obtained over a large range of h_1: the rf field amplitude must be large enough to reduce the signal height at the highest rf field to 50% or less of the maximum. We note that such conditions in an actual experiment are difficult to obtain from commercial instruments without added heating and drift: the use of large volume (TE_{102} or TM_{011}) EPR cavities requires ~1 W of power incident on the resonator to produce a 1 G rf field. LGRs are more suitable for this work as they can produce 1 G of rf field at ~0.1 W incident power (2).

Consider now the dependence of ϵ on the correlation time. ϵ was chosen as an adjustable parameter because it varied depending on lineshape and degree of inhomogeneity. The hypothesis that ϵ would be a valid monitor of the degree of inhomogeneity seems to be supported by the results (see Table 2). When the spectra consist of simple homogeneous first-derivative lines (i.e., fast-motion limit), then the rollover curves have an $\epsilon = 1.49 \sim$

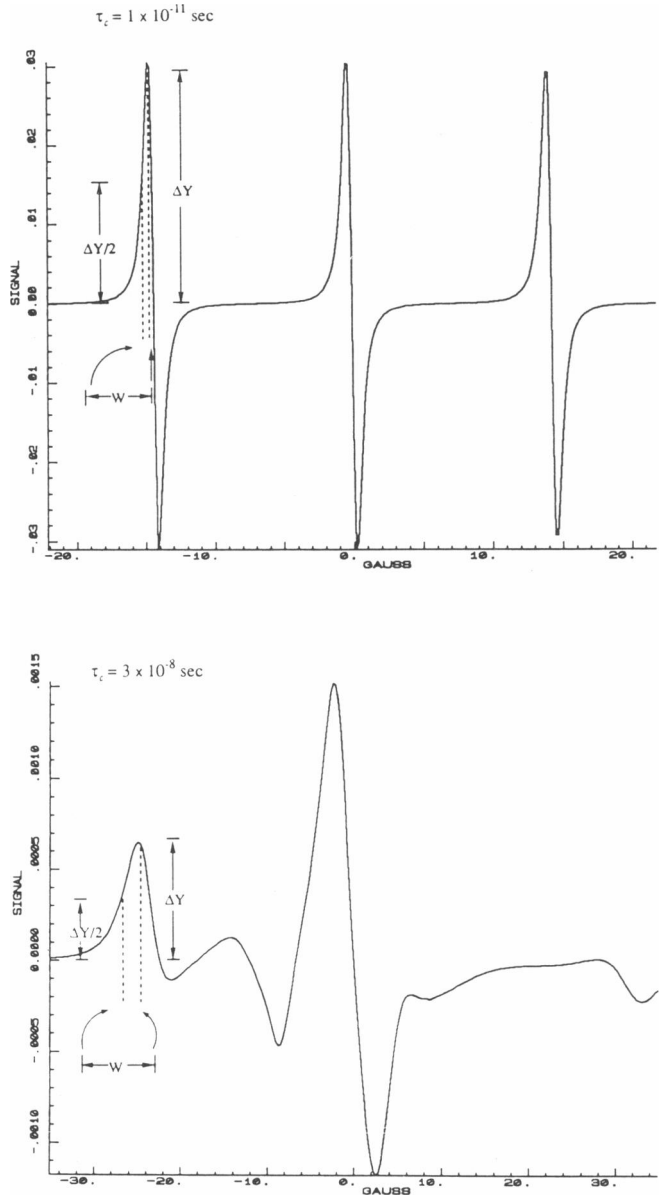

FIGURE 1 Simulated CW-EPR lineshapes for correlation times of $\tau_c = 10^{-11}$ s (fast motion) and $\tau_c = 3 \times 10^{-8}$ s (slow motion). The signal height for analysis, ΔY, is indicated on the spectra. Parameters used in the calculation were $g_x = 2.0086$, $g_y = 2.0066$, $g_z = 2.0032$, $A_x = A_y = 6.0$ G, $A_z = 31.0$ G, $T_{1e} = 1$ μs, $T_{2e} = 30$ ns, $h_1 = 0.04$ G.

3/2. As the motion slows, the value of ϵ decreases as expected. When the motion is on the order of 10 μs $\epsilon = 1.1$ to $1.2 \sim 1.0$ (as expected for the low field turning point in a pure homogeneous absorption shape). The value of ϵ at 30 ns motion is around 1.35 (still quite close to 3/2). This value of ϵ indicates that the line is still homogeneous at this correlation time even although the unsaturated CW-EPR spectrum has almost attained its rigid-limit lineshape.

In Fig. 3, P_2 is shown as a function of T_{1e}^{-1}, with the motional rate and other parameters held fixed. The excellent agreement of the simple-proportionality model with the values of P_2 strongly argues that P_2 can be realized as a product of T_{1e}^{-1} and R_2, each of which is independent of the other. Again, there is no reason a priori that the P_2 saturation rollover curve could be or should be interpretable in the simple fashion of Eq. 10; that it does we take as a fact based on our "computer experiments." This means that the rollover curve method of analysis allows one to extract values of T_{1e} under experimental conditions where R_2 remains constant. The changes in T_{1e} are exactly reflected in changes in P_2 (and qualitatively in $P_{1/2}$).

This was the situation encountered by Altenbach et al. (10) in their study of $P_{1/2}$ values from rollover curves. The spin labels on different residues all had R_2's between 10 and 100 Mrad/s. The broad linear EPR linewidths in this motional range should not be very sensitive to low levels of oxygen, a local paramagnetic relaxing agent, but T_{1e} should be. T_{1e} does change markedly when a spin label attached to an amino acid side chain is either in contact with the relatively oxygen-poor environment of the protein interior or the relatively oxygen-rich lipid membrane. Altenbach et al. (10) assumed that $P_{1/2}$ was

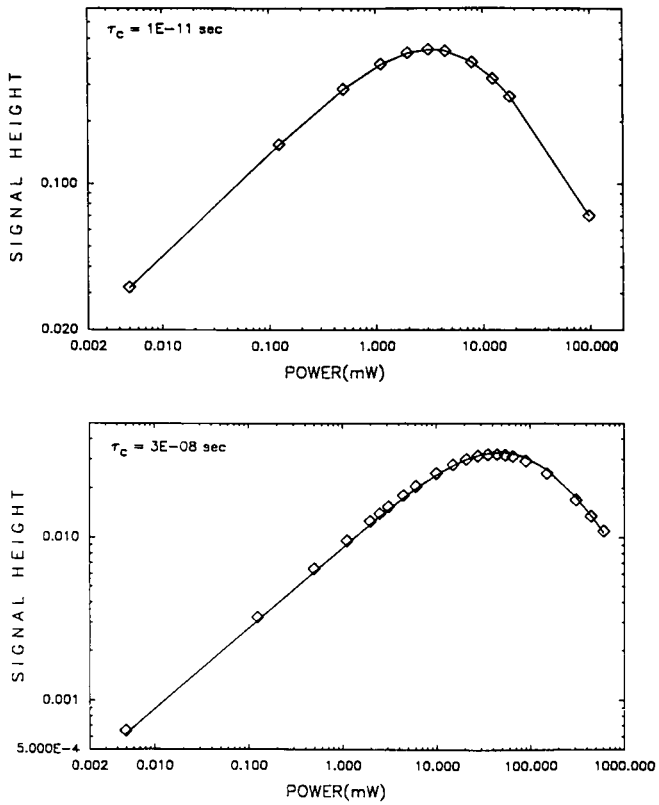

FIGURE 2 Plot of signal height ΔY versus the incident microwave power P_0 (commonly called "rollover" saturation curves) for the two simulated spectra of Fig. 1: correlation times $\tau_c = 10^{-11}$ s and $\tau_c = 3 \times 10^{-8}$ s. The solid lines are the fits of the simulated lineshapes to the equation for signal height ΔY versus power P_0 using Eq. 13. Fit parameters are given in Table 2.

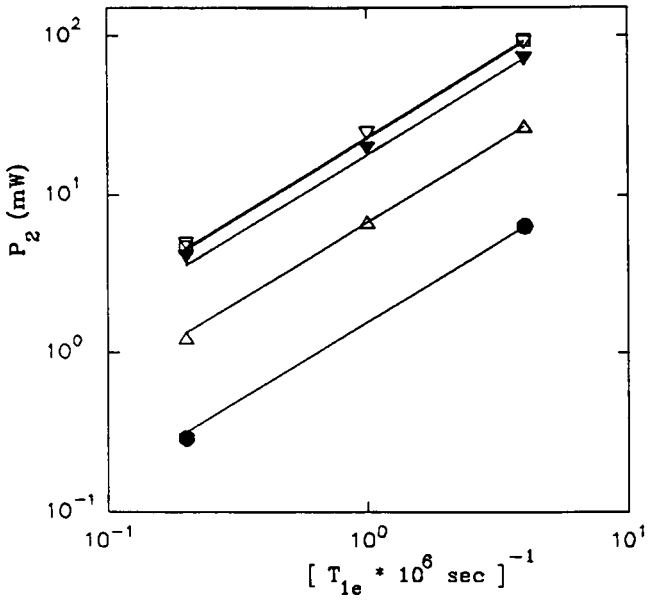

FIGURE 3 Plot of P_2 obtained from the rollover curves like those of Fig. 2 versus $1/T_{1e}$ for several correlation times. The values of T_{1e} were those entered into the simulation program. The various icons differentiate among P_2 values calculated using the following input parameters: $\tau_c = 10^{-11}$ s (*circles*); $\tau_c = 10^{-9}$ s (*triangles*); $\tau_c = 10^{-8}$ s (*squares*); $\tau_c = 3 \times 10^{-8}$ s (*inverted triangles*). In addition, hollow icons indicate T_{2e}^0 was 30 ns and filled icons indicate T_{2e}^0 was 100 ns. The solid lines are the best fit straight lines to the data.

inversely proportional to T_{1e}. Our theory shows that this is so provided ϵ does not change. At the correlation times used experimentally, ϵ is approximately independent of T_{1e} (Table 2), so that their assumption was justified. In general, plots of $P_{1/2}$ versus T_{1e}^{-1} would be slightly curved because, in fact, ϵ is a weak function of T_{1e} (Table 2). This complicates the agreement between changes in $P_{1/2}$ and changes in T_{1e}. However, $P_{1/2}$ can be determined more easily than P_2 from a rollover curve, and one is not required to go to large rf amplitudes; because ϵ is not able to be found accurately, a direct conversion to a valid T_{1e} is not possible.

The rollover curves of Fig. 2 show that P_2 (as well as P_{max}) is dependent on τ_c for fixed T_{1e}. In Fig. 2, the top curve (τ_c = 0.01 ns) is fit with P_2 = 6.3 mW and the bottom one (τ_c = 30 ns) is fit with P_2 = 71.0 mW, ~10 times greater. This is because R_2 is sensitive to τ_c.

The success of Eq. 12 may be contrasted with the failure of Eq. 8 to relate L^2 and P_0. Efforts to find a fitting function to linearize this relationship, that subsumed the effect of going from a derivative to an absorption shape, failed badly.

Fig. 4 shows the values of R_2 as a function of τ_c for different values of T_{1e} (see Table 2). In the top curve of Fig. 4, T_{2e}^0 = 30 ns, and on the bottom curve, T_{2e}^0 = 100 ns. The values of R_w, given in Table 2 and plotted on Fig. 4, provide a good estimate of R_2 (equivalent to $1/T_{2e}$) in the fast-motion limit. Also plotted are estimates of $R_{2e}(m)$ from Eq. 4 for $m = +1$ calculated from fast-motion theory given by Goldman (14) (*long, dashed line*), first-order modified fast-motion theory given by Hwang et al. (18) (*short, dashed line*), and a modified theory based on a generalized spectral density function (*solid line;* see Appendix). R_2 at slow correlation times is a measure of the effective homogeneous linewidth under saturation. We would expect that R_2 could not exceed a rate equivalent to the full linewidth of the low-field manifold, L_T (the distance between the z and y turning points). From Table 1 the value of L_T is 19.24 G (equal to 338 MRad/s as a rate). If the entire manifold were homogeneous with

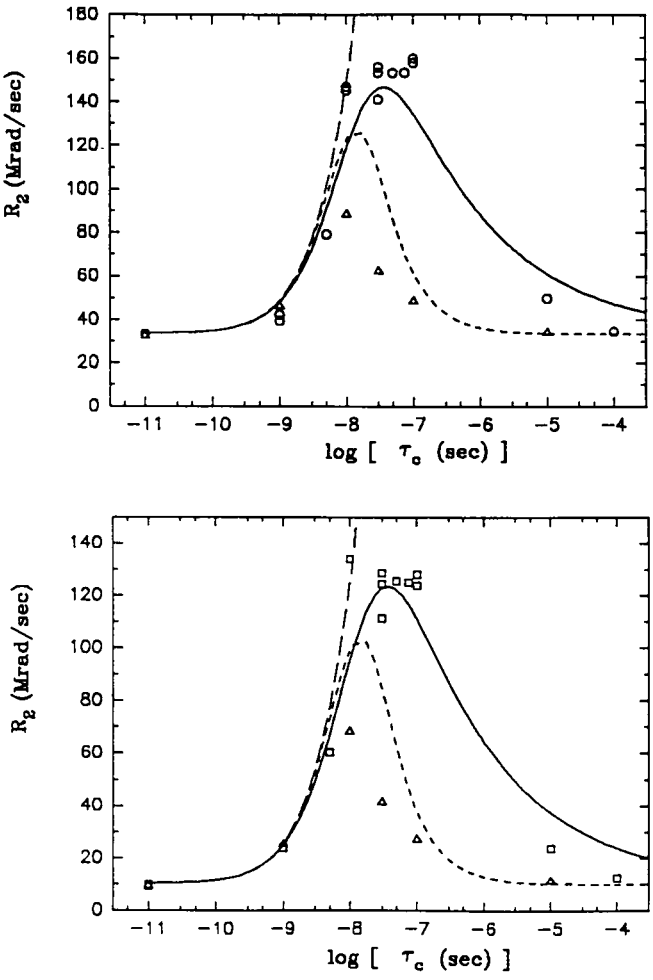

FIGURE 4 Plot of the value of $R_2 \equiv P_2 [(\gamma_e \alpha)^2 T_{1e}]$ versus correlation time, taken from column 7 of Table 2. (*Top*) R_2 (*open circles*) is plotted as a function of τ_c for the case where T_{2e}^0 = 30 ns and (*Bottom*) is the same as top except R_2 is represented by open squares and T_{2e}^0 = 100 ns. Also plotted is R_w (*open triangles*) (see Table 2) calculated from the measured linewidth, for comparison with R_2. The long dashed line is R_{2e} (Eq. 4 and Appendix) estimated by standard fast-motion theory ($\kappa = 0$, $\beta = 2$). The short dashed line is R_{2e} from the Hwang et al. (18) modified fast-motion theory ($\kappa = 1$, $\beta = 2$). The solid line is $R_{2e}(m)$ calculated from the modified spectral density function with κ = 1.0 and β = 1.3 (See Appendix).

this value of L_T, then the effective R_2 would be $L_T/2$. From Table 2 one can see that $L_T/2$ = 169 Mrad/s is a very reasonable upper bound for R_2.

Both R_2 and ϵ are independent estimates of the extent of homogeneity of the EPR spectrum under conditions of saturation and both show that the lines appear to retain a large amount of homogeneous character even when the motion is slow (on the linear EPR timescale). Under such conditions, the (partially) saturated lineshapes are sensitive to T_{1e} as already discussed. A practical consequence of this is found in the slow-motion ^{15}N spin-label study by Gaffney et al. (20). They observed broadening of the CW-EPR spectrum down to submicrosecond correlation times. We interpret this as an effect of saturation. As the motion slowed, T_{1e} lengthened so much so that the (fixed) observer power produced saturation. The slower the motion, the greater the degree of saturation, and hence the greater the line broadening (21).

We have established that a value of R_{2e} can be found from the simulations that enable one to calculate an accurate T_{1e}. It would be more satisfying to understand R_{2e} and how it varies with correlation time based on a more rigorous theory using spectral density functions. To illustrate the possible dependencies of R_{2e} (and R_2) on motion, we present a single, general spectral density function estimate for R_{2e} that subsumes some specific cases considered by others:

$$R_{2e} = \delta^2 \frac{\tau_c}{1 + (\kappa \times \delta \times \tau_c)^\beta} + \frac{1}{T_{2e}^0}. \qquad (14)$$

This form is consistent with fast-motion theory if $\kappa = 0$ and $\delta = [2/(3\sqrt{5})]\gamma_e L_T$ = 100 Mrad/s. The modified fast-motion theory of Hwang et al. (18) has $\kappa = 1$ and $\beta = 2$. (The full equations used for the calculations are given in the Appendix.)

Figure 4 shows that fast-motion theory values of R_{2e} ($m = 1$) are always larger than R_2 and those for the modified fast-motion theory are smaller than R_2. The modified fast-motion theory clearly avoids the (obviously incorrect) prediction that R_2 grows without bound as the motion slows. Although R_{2e} ($m = 1$) from the latter theory and R_w follow the same trend throughout the motional range, neither agrees well with R_2 from the saturation curve.

We now consider how R_2 is measured and why fast-motion theory cannot account for the observed values at correlation times slower than 5 ns. R_2 is obtained under conditions of maximum saturation. As such, features of the EPR spectrum are responding nonlinearly to the observer power, and the linewidths of the individual packets are being broadened. On the timescale determined by T_{2e}, only correlation times out to 300 ns can be detected. T_{1e} being on the microsecond timescale allows very slow rotation of the spin label (correlation times as great as 10 ms) to couple EPR resonance lines before the EPR signal decays (22).[3] The individual resonance lines are therefore in communication due to the motion on the timescale set by T_{1e}. In the slow-motion regime, at a fixed field–frequency position, there are many overlapping lines. In the absence of any motion, all lines relax with the same rate; when there is motion, the lines do not relax at the same rate because transfer of saturation competes with R_2 relaxation. This leads to a clustering of different relaxation rates about a mean. The theory that treats such a situation suggests that R_2 can be explained by the Cole–Davidson spectral density function in the frequency domain (or by a Williams–Watts stretched exponential function in the time domain) (23). The Cole–Davidson model has $1 < \beta < 2$, depending on the degree of spread of relaxation rates.

TABLE 3 Input parameters for simulations and parameters of rollover curve analysis

Input values			Results					
τ_c	T_{1e}	T_{2e}^0	ϵ	P_2	R_2	T_2	R_2^T	σ'
s	*μs*	*ns*		*mW*	*Mrad/s*	*ns*	*Mrad/s*	*G*
1E−11	0.25	30	1.25	29.0	45.56	21.9	79.9	0.77
1E−9	5	30	1.255	1.81	56.85	17.6	83.7	1.03
1E−8	5	30	1.167	4.67	146.7	6.81	168.9	0.0
1E−8	5	100	1.167	4.34	136.2	7.34	157.8	0.0
1E−7	5	30	1.292	5.53	173.6	5.67	178.7	1.71

Convolution = 2 G. All parameters have the same meaning as in Table 2; however, all simulations were convolved with a 2-G Gaussian broadening function and then analyzed by the rollover curve method for P_2 (and R_2) and ϵ, according to Eqs. 12 and 13. R_2^T was calculated from Eq. 16, where the Gaussian had σ = 2.0 G = 35.2 Mrad/s. σ' was calculated from Eq. 17.

Consider how β depends on the correlation time and T_{1e}. When τ_c is longer than T_{1e}, the flow of saturation between resonance lines ceases and $\beta = 2$. When the motion is faster than T_{1e}, the resonance lines are in communication, so $\beta < 2$. Conversely, if T_{1e} becomes smaller at a fixed correlation time, then β would become larger. Eq. 14 would therefore predict a slight decrease in R_2 if T_{1e} were shorter. Table 2 shows that this prediction is correct: a 20-fold change in T_{1e} produces only a few percent change in R_2. Therefore, even in the very slow motion region, P_2 can reasonably be interpreted as the product of R_2 and T_{1e}^{-1}.

The effects of protons (or deuterons) on the EPR spectrum have been simulated by a convolution with a Gaussian function of width σ. Generally σ spans the range from 0.2 to 2.8 G. Several sets of calculated lineshapes were convoluted with a Gaussian (σ = 2 G), and the saturation rollover curve of these spectra was analyzed

[3] See in particular Eq. 2.10 of Robinson et al (12).

according to Eq. 12. The results in Table 3 are rather surprising. The values of ϵ decreased in all cases, as expected, removing some of the effect on R_2 of the added inhomogeneity. Not all of the inhomogeneity was accounted for, and therefore the R_2 ($\sigma = 2$) was larger than the R_2 ($\sigma = 0$) for the corresponding set of lineshapes. Only for the spectra where τ_c was about 10 ns did it happen that the decrease in ϵ was just enough to keep R_2 constant. One can be more quantitative by considering the expression given by Bales (16) for the effects of Gaussian convolution, adapted to our notation:

$$\left(\frac{\sqrt{3}\sigma}{R_2(\sigma)}\right)^2 + \left(\frac{R_2(0)}{R_2(\sigma)}\right) = 1. \quad (15)$$

This relation shows that the resulting linewidth, $R_2(\sigma)$, can be estimated if one has a Lorentzian line, characterized by $R_2(0)$, that is convoluted by a Gaussian of width σ to give a Voightian lineshape. This relationship can be used to show how well the fitting function retrieves the original $R_2(0)$. Eq. 15 can be rearranged to solve for R_2 ($\sigma = 2$), called R_2^T, the total value one would expect if none of the convolution were removed:

$$R_2^T = R_2(0) \times \left\{\frac{1 + \sqrt{1 + 12(\sigma/R_2(0))^2}}{2}\right\}. \quad (16)$$

R_2^T (given in Table 3) would be expected to be an upper bound to R_2, and, presumably, if ϵ did not change, R_2^T would equal the R_2 extracted from the rollover fitting procedure. These expectations are borne out by the results in Table 3. Another way of viewing Eq. 15 is to rearrange it and solve for σ, called σ' (see Table 3), which is now an estimate of how much convolution was left behind after ϵ was adjusted and the fitting was optimized:

$$\sigma' = \sqrt{\frac{R_2(\sigma) \times [R_2(\sigma) - R_2(0)]}{3}}. \quad (17)$$

$R_2(\sigma)$ is the R_2 in Table 3 and $R_2(0)$ is the R_2 in Table 2 for the corresponding, nonconvoluted case. The conclusion is that when τ_c is <10 ns, σ is reduced by about a factor of 2. Because the amount of convolution is small (≤ 0.5 G) in this motional regime and half is removed, then the effects of Gaussian broadening are probably not going to affect estimates to P_2 and R_2. However, when τ_c is slower than 10 ns and the amount of broadening increases to around 2.8 G, considerable broadening remains. The results are clearly dependent on the motion. This finding is rather sobering for those who have used ϵ in the past to remove the effects of inhomogeneous broadening.

CONCLUSIONS

We have tested whether the simple idea of a saturation rollover curve, as given for a pure Lorentzian line, could be extended to estimate T_{1e} for nitroxide spin labels undergoing motion. The first, and most fundamental, result is that Eq. 9 gives a remarkably good accounting of the simulated lineshapes (e.g., Fig. 2) when ϵ is allowed to vary and be least-squares optimized. The second remarkable result is that P_2 is very nearly proportional to T_{1e}^{-1}. These two results mean that the method can be used to obtain meaningful estimates of P_2. Changes in P_2 reflect changes in T_{1e} under conditions where R_2 remains constant. As modifications to the experimental protocol, we recommend measuring saturation on the low-field turning point and using Eqs. 9 or 12, with variable ϵ to analyze the data. The method works well on the low-field line and does not work well on the center line. Measurements are made on the center line and analyzed but are not reported. Under some circumstances, $\epsilon > 1.5$ was found! This occurred because the outer lines overlapped the center one, and this increases with increasing h_1 due to broadening, raising the wings of the line to make it appear "super Lorentzian." Therefore, experimentally, one would be better off using the ^{15}N isotopically substituted analogue for the nitroxide spin label. Moreover, because ϵ does not remove Gaussian convolution very effectively, one is better off to use a fully perdeuterated ^{15}N spin label with the narrowest possible linewidth for careful quantitative studies.

T_{1e}^{-1} can be determined directly from spectral simulation: the A- and g-tensors, as well as T_{2e}^0, σ, and the motional rate, are all determined from the linear CW-EPR lineshape. T_{1e} is only one unknown parameter remaining to be quantitatively determined from the rollover curve. Of course, rollover curves also can be simulated, using the programs that are derived from Eq. 1, varying T_{1e} until optimal agreement is found.

This process may be avoided by rearranging Eq. 13 for T_{1e}:

$$T_{1e}^{-1} = P_2(\gamma_e\alpha)^2/R_2. \quad (18)$$

Quantitative estimates of T_{1e} can be obtained using the values of P_2, determined from the experimental rollover curve, and R_2, generated by simulation or taken from Table 2. Methods for determining α are described elsewhere (2). We have considered in detail the parameters that affect R_2 and to what degree R_2 is a valid description of the homogeneous linewidth under saturation.

We argue that R_2 has validity in its own right, even though there is no simple a priori formula to determine it. The first point is that R_2 is the same as that predicted by fast-motion theory in the regime where that theory is valid. The second point is that R_2 is qualitatively described by the Hwang et al. (18) modified fast-motion theory over the entire motional range of interest. For example, at maximum R_2, modified fast-motion theory underestimates R_2 by only $\sim$20%. The third point is that Table 2 and Fig. 4 demonstrate that R_2 is a very weak function of T_{1e}^{-1}. The fourth and final point is that it is

plausible that the plateau of R_2 between 10 and 200 ns may be accounted for by a motion-dependent β. Despite the limitations that have been pointed out in the discussion, Fig. 4 may be used to obtain a first-order estimate to R_2.

For rotational times faster than 5 ns, R_2 may be estimated quite accurately from the fast-motion equations given in the Appendix. For rotational times from 10 to 200 ns, R_2 is rather insensitive to motion. This then should be the optimal motional regime for obtaining T_{1e} by progressive saturation. For motions slower than a microsecond, ST-EPR spectra are directly sensitive to T_{1e} and can be directly compared (or simulated) to estimate T_{1e} (24).

We note that when $\omega_m T_{1e} > 1.0$, then the DC field modulation can affect the value of T_{1e} experimentally obtained (see Eq. 6). Based on direct measurements of T_{1e} with saturation recovery pulsed EPR (25), this condition is violated for motions slower than 0.1 ns when 100-kHz field modulation is used. It is therefore advisable that a modulation frequency much less than this be used in experiments with slower moving molecules.

APPENDIX

The equation for $R_{2e}^G(m)$ is given below. This was originally given in Goldman et al. (14) and later modified in Hwang et al. (18). It is further modified below to include a generalized spectral density function.

$$R_{2e}^G(m) = A(m) + mB(m) + m^2C(m),$$

where $A(m)$, $B(m)$, and $C(m)$ depend on m, which takes on the values $m = 0, \pm 1$ for ^{14}N. The following formulae are valid only for ^{14}N where $I = 1$. These equations are identical to those in Goldman et al. (14) when $\kappa = 0$ and $\beta = 2$ and reduce to the A, B, and C parameters defined therein and are identical to those in Hwang et al. (18) when $\kappa = 1$ and $\beta = 2$.

$$A(m) = \frac{I(I+1)}{5}\sum_{j=0}^{2}\left(1+\frac{j}{2}\right)(D_j)^2 \times\left\{\frac{1}{2}\left[J_{j,\beta}(\omega_j^+(m)) + J_{j,\beta}(\omega_j^-(m))\right] + \frac{7}{3}J_{j,2}(\omega_e)\right\} + \frac{2}{5}\sum_{j=0}^{2}\left(1+\frac{j}{2}\right)(G_j)^2\left\{\frac{1}{3}J_{j,\beta}(\omega_3(m)) + \frac{1}{4}J_{j,2}(\omega_e)\right\},$$

$$B(m) = \frac{2}{5}\sum_{j=0}^{2}\left(1+\frac{j}{2}\right)(G_jD_j)\left\{\frac{4}{3}J_{j,\beta}(\omega_3(m)) + J_{j,2}(\omega_e)\right\},$$

$$C(m) = \frac{1}{5}\sum_{j=0}^{2}\left(1+\frac{j}{2}\right)(D_j)^2 \times\left\{\frac{8}{3}J_{j,\beta}(\omega_3(m)) - J_{j,\beta}(\omega_j^m(m)) - \frac{1}{3}J_{j,2}(\omega_e)\right\}.$$

The sum over j is only for $j = 0$ and $j = 2$. $C(m)$ is not defined, or needed, for $m = 0$. The generalized spectral density function is:

$$J_{j,\beta}(\omega) = \frac{\tau_j}{1+(\omega\tau_j)^\beta},$$

and is valid for $j = 0$ and 2 only. $\tau_0 = 1/6d_\perp$ and $\tau_2 = 1/(2d_\perp + 4d_\parallel)$, where $d_\parallel$ and $d_\perp$ are the Einstein diffusion coefficients for rotation of an axially symmetric object about its unique axis and perpendicular to the unique axis, respectively. These equations assume that the D (diffusion) and g and A tensors are all coincident. $\omega_e = \gamma_e H_0$, where ω_e is the electron Larmor frequency and $\omega_a = \gamma_e\bar{a}/2$.

The other frequencies used constitute the various possible linear combinations associated with the manifold separations and widths:

$$\omega_j^{\pm}(m) = \left|\omega_a + (-1)^{(1+j/2)}\left[\pm F_0 + (-1)^m\frac{D'}{2}\right]\frac{\kappa}{7}\right|,$$

and

$$\omega_3(m) = \left|\frac{2\kappa}{7}(F_0 + mD')\right|.$$

The elements of D and G are:

$$D_0 = \frac{1}{\sqrt{6}}\gamma_e\left[A_z - \frac{1}{2}(A_x + A_y)\right]$$

$$G_0 = \frac{1}{\sqrt{6}}\omega_e\left[g_z - \frac{1}{2}(g_x + g_y)\right],$$

$$D_2 = \frac{1}{4}\gamma_e(A_x - A_y) \quad G_2 = \frac{1}{4}\omega_e[g_x - g_y],$$

$$D' = \frac{2}{3}\gamma_e\left[A_z - \frac{1}{2}(A_x + A_y)\right]$$

$$F_0 = \frac{2}{3}\omega_e\left[g_z - \frac{1}{2}(g_x + g_y)\right]\Big/\bar{g}.$$

D_0 and D_2 are multiplied by 2π as compared with D_0 and D_2 defined by Goldman et al. (14). G_0 and G_2 are multiplied by $\omega_e/2$ as compared with the G_0 and G_2 defined by Goldman et al. (14).

To investigate how the generalized spectral density function of Eq. 14 could account for the observed values of R_2, κ was set equal to one, various values of β were chosen, and the resultant R_{2e} curves were overlaid on the data. Having $\beta < 2$ produces a broader maximum, but if β is set equal to unity, R_{2e} reaches a maximum and remains constant at longer τ_c. No attempt was made to make β a function of τ_c or T_{1e}, as would be necessary in a complete treatment. The estimate of $R_{2e}^G(m)$ using $\beta = 1.3$ (*solid line*, Fig. 4) shows that Eq. 14 can give a reasonable explanation of the dependence of $R_{2e}^G(m)$ (and by implication R_2 as well).

The authors acknowledge the support of the Natural Sciences and Research Council of Canada and the National Institutes of Health.

Received for publication 5 October 1992 and in final form 19 November 1992.

REFERENCES

1. Poole, C. P. 1972. Electron Spin Resonance: A Comprehensive Treatise on Experimental Techniques. 2nd ed. Wiley, New York. 992 pp.
2. Mailer, C., D. A. Haas, E. J. Hustedt, J. G. Gladden, and B. H. Robinson. 1991. Low power EPR spin-echo spectroscopy. *J. Magn. Reson.* 91:475–496.
3. Czoch, R., and A. Francik. 1989. Instrumental Effects in Homodyne Paramagnetic Resonance Spectrometers. Ellis Horwood Ltd. New York. 395 pp.

4. Castner, T. G. 1959. Saturation of the Paramagnetic Resonance of an F-Center. *Phys. Rev.*, 115:1506.
5. Metz, H., G. Volkel, and W. Windsch. 1990. A Simple Method for Fitting of Inhomogeneous ESR Saturation Curves. *Phys. Status Solidi A*, 122:K73–K76.
6. Bowman, M. K., H. Hase, and L. Kevan. 1976. Saturation Behavior of Inhomogeneously Broadened EPR Lines Detected with Magnetic Field Modulation. *J. Magn. Reson.*, 22:23–32.
7. Clough, S., and C. A. Scott. 1968. Saturation and spectral diffusion in ESR. *J. Phys. Chem.* 1:919–931.
8. Freed, J. H., G. V. Bruno, and C. F. Polnaszek. 1971. ESR Lineshapes and Saturation in the Slow Motional Region. *J. Phys. Chem.* 75:3385–3399.
9. Freed, J. H. 1976. Theory of slow tumbling ESR spectra for nitroxides. *In* Spin Labelling: Theory and Application. Vol. I. L. J. Berliner, editor. Academic Press, New York. 53–132.
10. Altenbach, C., S. L. Flitsch, H. G. Khorana, and W. L. Hubbell. 1989. Structural Studies on Transmembrane Proteins 2. Spin Labelling of Bacteriorhodopsin Mutants at Unique Cysteines. *Biochemistry.* 28:7806–7812; and Altenbach, C., S. L. Flitsch, H. G. Khorana, and W. L. Hubbell. 1990. Transmembrane Protein Structure: Spin Labelling of Bacteriorhodopsin Mutants. *Science (Wash. DC).* 248:1088–1092.
11. Dalton, L. R., B. H. Robinson, L. A. Dalton, and P. Coffey. 1976. Saturation Transfer Spectroscopy, Advances in Magnetic Resonance. Vol. 8. J. S. Waugh, editor. Academic Press, New York. 149–259.
12. Robinson, B. H., H. Thomann, A. H. Beth, P. Fajer, and L. R. Dalton. 1985. The phenomenon of magnetic resonance: Theoretical considerations. *In* EPR and Advanced EPR Studies of Biological Systems. L. R. Dalton, editor. CRC Press, Boca Raton, FL. 1–314.
13. Redfield, A. G. 1965. Theory of relaxation processes. *In Advances in Magnetic Resonance.* Vol. I. J. S. Waugh, editor. Academic Press, New York.
14. Goldman, A., G. V. Bruno, C. F. Polnaszek, and J. H. Freed. 1972. An ESR Study of Anisotropic Reorientation and Slow Tumbling in Liquid and Frozen Media. *J. Chem. Phys.* 56:716–735.
15. Beck, W. F., J. B. Innes, J. B. Lynch, and G. W. Brudvig. 1991. Electron Spin-Lattice Relaxation and Spectral Diffusion Measurements on Tyrosine Radicals in Proteins. *J. Magn. Reson.* 91:12–29.
16. Bales, B. 1989. Inhomogeneously broadened spin-label spectra. *In* Biological Magnetic Resonance. Vol. 8.—Spin Labeling: Theory and Applications. L. J. Berliner and J. Reuben, editors. Plenum Press, New York.
17. Beth, A. H., K. Balasubramanian, B. H. Robinson, L. R. Dalton, and S. D. Park. 1983. Sensitivity of ST-EPR Signals to Anisotropic Diffusion with ^{15}N Nitroxide Spin Labels. Effects of Noncoincident Magnetic and Diffusion Tensor Principal Axes. *J. Phys. Chem.* 87:359–367.
18. Hwang, J. S., R. Mason, L. P. Hwang, and J. H. Freed. 1975. ESR Studies of Anisotropic Rotational Reorientation and Slow Tumbling in Liquid and Frozen Media. III. Perdeuterated 2,2,6,6-Tetramethyl-4-piperidone N-Oxide and an Analysis of Fluctuating Torques. *J. Phys. Chem.* 79:489–511.
19. Beth, A. H., and B. H. Robinson. 1989. Nitrogen-15 and deuterium substituted spin labels for studies of very slow motional dynamics. *In* Spin Labeling: Theory and Applications. *Biological Magnetic Resonance.* Vol. 8.—Spin Labeling: Theory and Applications. L. J. Berliner and J. Reuben, editors. Plenum Press, New York. 179–253.
20. Gaffney, B. J., C. H. Elbrecht, and J. P. A. Scibilia. 1981. "Enhanced Sensitivity to Slow Motions using ^{15}N-Nitroxide Spin Labels," *J. Magn. Reson.* 44:436–446.
21. Robinson, B. H., and L. R. Dalton. 1979. "EPR and Saturation Transfer EPR Spectra at High Microwave Field Intensities," *Chem. Phys.* 36:207–237.
22. McConnell, H. M. 1975. Molecular motion in biological membranes. *In* Spin Labeling: Theory and Applications. Vol. I. L. J. Berliner, editor. New York. 525–561.
23. Lindsay, C. P., and G. D. Patterson. 1980. "Detailed Comparison of the Williams-Watts and Cole-Davidson Functions," *J. Chem. Phys.* 73:3348–3357.
24. Robinson, B. H. 1983. "Effects of Over-Modulation on Saturation Transfer EPR Signals," *J. Chem. Phys.* 78:2268–2273.
25. Mailer, C., B. H. Robinson, and D. A. Haas. 1992. "New Developments in Pulsed EPR. Relaxation Mechanisms of Nitroxide Spin Labels," *Bull. Magn. Reson.* 14:30–35.